

INFLUENCE OF MICROALLOYING AND THE THERMOMECHANICAL METHOD OF PROCESSING ON THE COMMUNUTION OF THE COPPER STRUCTURE

VPLIV MIKROLEGIRANJA IN TERMOMEHANSKIH POSTOPKOV PROCESIRANJA NA SPREMEMBE MIKROSTRUKTURE BAKRA

Milijana Mitrović^{1*}, Biserka Trumić², Saša Marjanović¹, Mirjana Šteharnik²,
Vesna Krstić^{1,2}

¹University of Belgrade, Tehnical Faculty in Bor, Vojske Jugoslavije 12, Bor, Serbia

²Mining and Metallurgy Institute Bor, Zeleni bulevar 35, Bor, Serbia

Prejem rokopisa – received: 2024-04-26; sprejem za objavo – accepted for publication: 2024-11-07

doi:10.17222/mit.2024.1171

Copper, as a basic element, was alloyed with iron (Fe) and phosphorus (P). This paper presents the results of the copper structure comminution in the Cu-Fe-P alloy, with the chemical composition containing 0.003 w/% and 0.014 w/% of Fe and P, respectively, and with certain mechanical and structural characteristics. A homogeneous Cu-Fe-P alloy was synthesized to generate certain mechanical and structural properties, meeting the strict requirements of industry. These requirements refer to Vickers hardness (HV10) which should be from 45 to 70, tensile strength (R_m) with a minimum of 230 N/mm², relative elongation (A) with a minimum of 40 %, and number of grains (K_z) of around 4000 grains/mm². In order to achieve the required conditions, a series of samples of the mentioned alloy were tested. Molten, chemically homogenized material was subjected to an extrusion process. Also, to achieve the above characteristics, cold processing (rolling) was used with deformation degrees of (10, 30, 50, 75, 80) %. Recrystallization annealing, for the purpose of creating a fine-grained structure, was done at 450 °C in a protective atmosphere of nitrogen and hydrogen, with annealing times of (35, 90, and 150) min. The results indicated that optimal conditions for the required mechanical and structural characteristics of the material were achieved at a deformation degree of 80 %, an annealing time of 150 minutes and a temperature of 450 °C.

Keywords: Cu-Fe-P, microalloying, plastic processing, mechanical and structural characteristics

Avtorji v članku opisujejo legiranje bakra (Cu) z železom (Fe) in fosforjem (P) ter opisujejo rezultate mehanskih in mikrostrukturnih lastnosti izdelane Cu-Fe-P zlitine z 0,003 w/% Fe in 0,014 w/% zaradi mikrostrukturnih sprememb (udrobljenja). Homogeno Cu-Fe-P zlitino so avtorji sintetizirali tako, da je izpolnjevala vse mehanske in mikrostrukturne lastnosti, ki so zahtevane za njeno točno določeno industrijsko uporabo. Zahteve se nanašajo na njeno mehansko trdoto po Vickersu (HV10), ki mora biti med 45 in 70, njeno minimalno natezno trdnost (R_m) 230 N/mm², minimalni relativni raztezek (A) 40 % in število kristalnih zrn (K_z) okoli 4000 zrn/mm². Zato, da bi avtorji dosegli zahtevane lastnosti zlitine so izdelali in testirali serijo preizkušancev. Raztaljen, kemijsko homogeniziran material so po ohlajanju ekstrudirali. Prav tako so izvedli tudi hladno valjanje zlitine z različno stopnjo hladne deformacije (30, 50, 75, in 80) %. Sledilo je rekristalizacijsko žarjenje pri 450 °C v zaščitni atmosferi dušika in vodika z namenom formiranja fino zrnate mikrostrukture. Rekristalizacijsko žarjenje so izvajali različno dolgo časa (35, 90 in 150) min. Rezultati preiskav so pokazali, da so dosegli zahtevane mehanske in mikrostrukturne lastnosti Cu-Fe-P zlitine z izbrano kemijsko sestavo pri 80 %-ni stopnji deformacije in času rekristalizacijskega žarjenja 150 min na temperaturi 450 °C.

Ključne besede: Cu-Fe-P, mikrolegiranje, plastično procesiranje, mehanske in mikrostrukturne lastnosti.

1 INTRODUCTION

Only a small concentration of Fe added to pure Cu significantly changes the characteristics of Cu and meets different needs, depending on the application. In addition to Fe, other elements can be added to Cu, such as Mo, Pb, Co, Ti, W, Cr, Zr, Ni, Si, etc., and new properties of Cu can then be investigated. Cu and Cu alloys have excellent mechanical properties, as well as thermal and electrical conductivity. For this reason, the need for the production, processing, and application of these alloys in

a wide area of industry has significantly increased in recent years.¹⁻³

The development of techniques for the production of materials with specific characteristics must be accompanied by new processing technologies that, in addition to high productivity, should also ensure high quality. Therefore, it is not easy to choose the appropriate thermomechanical regime for the processing of such materials, when certain values of mechanical and structural characteristics are pre-defined according to industry requirements. Cu-Fe alloys can be obtained using different methods. Thus, Zou et al., obtained the Cu-14Fe composite through casting under an alternating magnetic field,² while Wang et al. obtained Cu-10 wt% Fe alloy using double-melt mixed casting and multi-stage thermomechanical treatment.³ Jang et al. examined the

*Corresponding author's e-mail:
mmitrovic@tfbor.bg.ac.rs (Milijana Mitrović)



© 2024 The Author(s). Except when otherwise noted, articles in this journal are published under the terms and conditions of the Creative Commons Attribution 4.0 International License (CC BY 4.0).

strength and electrical conductivity achieved by optimizing the dual-phase structure of Cu–Fe wires.⁴ The authors analyzed the influence of microstructural parameters on the mechanical properties and electrical conductivity of wires. Annealing the alloy at 500 °C led to the precipitation of Cu nanoparticles in the Fe-phase and Fe in the Cu-phase. The result of wire drawing deformation significantly improved the strength of the wires, while the electrical conductivity was not significantly reduced.⁴ Ding et al. obtained the Cu–Fe composite by vacuum casting,⁵ while Tian et al. used the powder rolling method.⁶ Li et al. produced a hierarchical microstructure and strengthening mechanism of Cu-36.8Fe alloy with selective laser melting.⁷ One of the frequent methods of obtaining the Cu-Fe alloy is using metal powders.^{8–10}

One of the important required structural characteristics is the grain refinement of Cu and Cu alloys.^{11,12} Thus, Feng et al. investigated the effect of casting and crystallization temperature on the grain refinement of pure Cu hardened by means of a pulsed magnetic field at low pressures.¹³ Higher casting and crystallization temperatures resulted in lower cooling rates, providing a longer time for counteracting the effects of the pulsating magnetic field, thereby achieving a better grain refinement.¹³ Zaher et al. investigated the effects of Sn and strain rate on the grain refinement and defects in severely deformed Cu.¹⁴ In their study, it can be seen that the addition of Sn significantly reduces the grain size, while a higher degree of deformation reduces the grain size and increases the density of defects in CuSn8 alloys.¹⁴ Chen et al. applied a simple and effective powder sintering procedure to obtain these materials, but they were easily deformed and had a poor finish.¹⁵ On the other hand, according to Fang et al., materials produced by electrolytic deposition techniques have higher density and finer grain, but lower production capacity.¹⁶

The above researches provide information about new methods of obtaining materials and contribute to a better understanding of the grain refinement mechanism in copper alloys.

Since in Cu-Fe alloys, during severe plastic deformations, a large number of dislocations are formed, which favor the precipitation of Fe atoms in the alloy, Zhang et al. explained that an addition of alloying elements reduced the interphase energy of Fe atoms in a solid solution with Cu, thereby promoting the precipitation of Fe from the solid solution. That way, attention was drawn to microalloying.¹⁷ Wang et al. indicate that the presence of Fe up to 5 w/% positively affects the mechanical properties of Cu alloys.¹⁸ Due to the low solubility of Fe in Cu, an uneven distribution of the Fe-phase occurs during solidification of Cu-Fe alloys, which leads to serious macrosegregation that worsens the performance of Cu-Fe alloys.^{19,20} Wang et al. pointed out that Cu-Fe alloys with a relatively uniform composition and uniform structure,

especially alloys with the Fe content higher than 5 %, are difficult to prepare with the traditional casting method.²¹

An addition of non-metals such as P significantly affects the properties of Cu. The solubility of P in Cu is low and it is used primarily as a strong deoxidizing agent. With an increase in the P content, the area of Cu superplasticity expands because P, as an active interfacial component, prevents sudden grain growth and thus improves the technological properties during plastic processing. However, experience has shown that with an increase in the P content above 0.4 w/% and an increase in the casting speed, the quality of the casting surface deteriorates sharply.²² Wang et al. showed that the P content in steel must be controlled and should be below 0.045 w/%.²³ However, P, whether present as an impurity or in trace amounts, is an effective scavenger of oxygen in cast copper. It can also improve the fluidity of Cu, which gives an alloy excellent mechanical and electrical properties.¹⁷

The research presented in this paper aimed to analyze the influence of a certain thermal annealing regime, and mechanical regimes of processing on the mechanical and structural characteristics of microalloyed copper. The tested copper alloy had to meet the requirements including a hardness (HV10) of 45–70, a minimum tensile strength (R_m) of 230 N/mm², a minimum relative elongation (A) of 40 %, and a number of grains (K_z) of around 4000 grains/mm². Tests were first performed in laboratory conditions and then continued in semi-industrial conditions.

2 EXPERIMENTAL PART

2.1 Materials and techniques

To obtain the Cu-Fe-P alloy, cathodic Cu with a 99.99 % purity was used (grade A quality produced by AURUBIS, Bulgaria). The melting of Cu cathodes was carried out in an electrical resistance furnace with a protective atmosphere, and the casting of the alloy was carried out using upward casting, **Figure 1a**.

Cu microalloying was performed by adding the CuP6.42 prealloy, while Fe was added in the powder form.

The obtained microalloyed Cu rod was subjected to multiple remelting cycles after casting to achieve better homogenization. Control of the chemical composition of the synthesized alloy was carried out continuously by examining a sample every hour of the casting. The content of Fe and P was determined with an optical emission spectrometer with spark excitation (OES) (manufactured by ARL, model 4460, USA). The cast rods, with a diameter of 20 mm and a satisfactory chemical composition, were then transferred to the extrusion device. There, strips with a 150 mm width and 19.8 mm thickness were obtained, **Figure 1b**. Samples were prepared from these strips, which were interphase annealed in an electric resistance furnace (manufactured by Instrumentaria

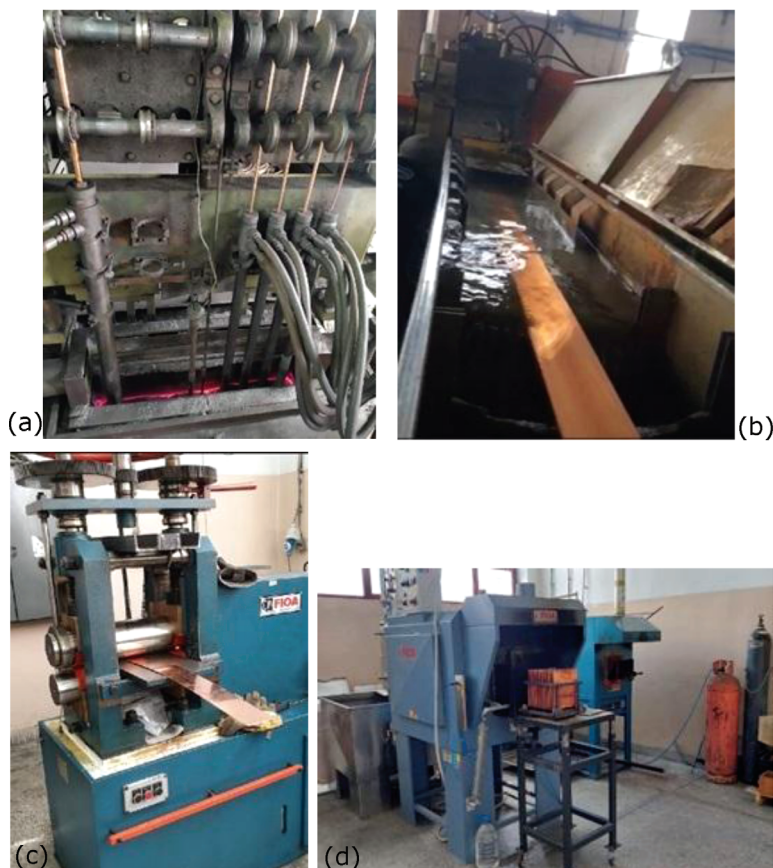


Figure 1: View of the plant: a) upward casting of the microalloyed copper rod, b) extrusion procedure, c) rolling mill with smooth rollers, and d) annealing furnace

Zagreb, Croatia) at 550 °C for 30 min. After annealing, all samples were tempered in a mixture of water and ethyl alcohol.

Cold plastic processing involved rolling of samples on a rolling mill with smooth rollers (manufactured by FIOA, Italy), **Figure 1c**, at different degrees of deformation of (10, 30, 50, 75, and 80) %. To eliminate the impact of sample thickness on the alloy properties,²⁴ all samples were planned to have a uniform thickness of 4 mm. Based on the final thickness and final degrees of deformation, the pre-final thickness values of the samples were calculated. Before the final rolling, the samples were annealed at 550 °C for 30 min in an electric resistance furnace to eliminate deformation stress. After annealing and tempering the samples in a mixture of water and ethyl alcohol, the final rolling was performed, resulting in strips with a thickness of 4 mm.

The final recrystallization annealing of the samples was conducted in a chamber electric resistance furnace (manufactured by FIOA, Italy). The annealing was carried out at 450 °C in a protective atmosphere of nitrogen (5 % purity) and hydrogen (5 % purity) for durations of (35, 90, and 150) min. The furnace was directly linked to the sample cooling chamber. The samples were cooled in a mixture of water and 96 % ethyl alcohol in a ratio of 3:1, **Figure 1d**.

The hardness of the samples was determined using the Vickers method on the hardness tester device (manufactured by VEB-LEIPZIG, Germany), with a load of 10 kg and a load duration of 15 s. The hardness values represent the average of 8 to 10 measurements, conducted both along and across the rolling direction.

The measurements of the tensile strength and elongation of the samples were performed on a tear machine (manufactured by KARL FRANK, Germany, model 81 221-12).

Metallographic preparation of the samples was conducted using an electrolytic polishing and etching device, (manufactured by METKOM ELOPREP, Turkey, model 102). An aqueous solution of 85 % phosphoric acid and 96 % ethyl alcohol (250 mL phosphoric acid, 250 mL ethyl alcohol, and 250 mL distilled water) was used as the electrolyte for polishing the samples, with a polishing time of 60 s for each sample. The polished samples were additionally etched using an aqueous solution of 96 % ferric chloride and 96 % hydrochloric acid (1 g ferric chloride, 3 mL hydrochloric acid, and 20 mL distilled water) for 35 s, after which they were rinsed with distilled water.

Microstructural analysis of the prepared samples was performed on an optical microscope (OM), (manufactured by LEICA, Germany, model DM 2700M),

Table 1: Chemical composition of Cu-Fe-P alloy

Element	Cu	P	Fe	Si	Pb	Se	S	Ag	Cr	Mn
w/%	99.98	0.0139	0.0028	0.0012	0.0002	0.0001	0.001	0.0009	0.0001	0.0001

equipped with a Flexcam – C1 digital camera. Grain counting was performed using the Leica Grain & Phase Expert image analysis software following the planimetric method from the STM E112-10 standard.²⁵ To determine the average number of grains, in accordance with the requirement of the standard, 3 to 5 representative areas were measured at a magnification of 100× on each examined sample.

X-ray analysis was performed using a Rigaku MiniFlex 600 with a D/teX Ultra 250 high-speed detector and a Cu anode X-ray tube. The range of angles was 3–90°, the step was 0.02°, the recording speed was 10°/min, with 40 kV and 15 mA. The identification of the samples was made with the PDXL 2 Version 2.4.2.0. software, and the ICDD database (PDF-2 Release 2015 RDB). The detection limit was 1 %.

The surface appearance was investigated with SEM (JEOL, JSM IT 300LV) and EDS (OXFORD Instruments).

2.2 Methods

The solubility of Fe in Cu is low. It reaches a maximum of 3.5 % at a temperature of 1050 °C and decreases as the temperature decreases, so that at 635 °C it is only 0.15 %.¹⁷

P was added to allow deoxidation, increase the fluidity and make the alloy easier to process.²⁶

The extruded pieces were rolled with varying degrees of deformation of (10, 30, 50, 75, 80) %, up to a final thickness of 4 mm for the copper plates. The samples were marked according to XXDD-YY, where DD stands for the Degree of Deformation, XX (%) represents the value of DD, and YY (min) determines the annealing duration of each sample. XX corresponds to the values of (10, 35, 50, 75, 80) % DD, while YY corresponds to the times of (35, 90, 150) min, which are the annealing dura-

tions at 450 °C for each of the above deformations. In other words, the general marking system of the prepared and tested samples is 10÷80DD-35÷150, while the individual marking system is, for example, 80DD-150.

After each degree of deformation, mechanical characteristics such as Vickers hardness (HV10), tensile strength (R_m), and relative elongation (A) were examined. In addition to Fe as an alloying element, the extrusion process and cold plastic processing, i.e., rolling of the already extruded material, play a major role in the comminution of the structure.²⁷

Changes in the mechanical and physical properties of the Cu-Fe alloy, compared to pure Cu, are to the greatest extent a consequence of the influence of the Fe content on the microstructure. The addition of Fe to Cu affects the density and arrangement of dislocations, the rate of dynamic recovery, recovery, recrystallization, and thus the resulting grain size and texture.

3 RESULTS AND DISCUSSION

In order to obtain a Cu-Fe-P alloy with predetermined characteristics, the influence of the thermomechanical processing regime on the achievement of the mechanical and structural characteristics of the Cu-Fe-P ternary system alloy was examined. Fe and P were used as alloying elements in concentrations of 0.003 w/% and 0.014 w/%, respectively. The results of the analysis of the chemical composition of the synthesized alloy are presented in **Table 1**.

The XRD diagram for the Cu-Fe-P alloy with an 80 % deformation degree is shown in **Figure 2**. The result shows that Cu-Fe-P alloy has Cu diffraction peaks corresponding to pure Cu and copper oxide (Cu₂O). Diffraction lines for Cu are shown by peaks at angles of 42.91°, 51.84°, and 74.96° of 2 θ corresponding to reflections of Cu from (111), (200), and (220), respectively. Considering the detection limit of the instrument, there were no diffraction peaks corresponding to Fe and P or their potential compounds. Unlike the results we obtained on the diffractogram where all peaks correspond to pure Cu for the Cu-Fe-P alloy, Zhang et al.¹⁷ analyzed a series of Cu-20Fe-xP alloys, in which the Fe concentration was constant, being 20 w/%, and the P concentration varied in a range of 0.05–1.0 w/%. With the concentration of Fe and P in the alloy, peaks corresponding to the Fe₃P compound with reflections (321) and (411), and the α -Fe phase corresponding to reflections (110) and (200) appear on their diffractogram. Low-intensity peaks corresponding to Cu₂O indicate the beginning of oxidation due to the nature of the material.

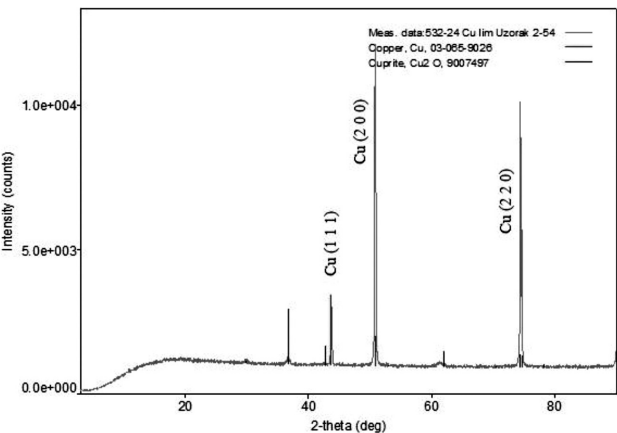


Figure 2: XRD analysis of Cu-Fe-P alloy with 80DD-150

Figure 3a shows the microstructure of a rod obtained with upward casting. The grains are relatively large due to slow hardening, and grains are directed towards the crystallization axis, which is strictly in the center of the casting. The extrusion process takes place under the influence of active friction that occurs between the work-piece and the working wheel. As the wheel rotates, it pulls the rod into the charging chamber, where, due to high compressive stresses and shear deformation, the metal is being heated. The temperature in the deformation zone can reach between 450 °C and 600 °C, resulting in dynamic recrystallization and significant comminution of the grains during extrusion, **Figure 3b**.^{28,29}

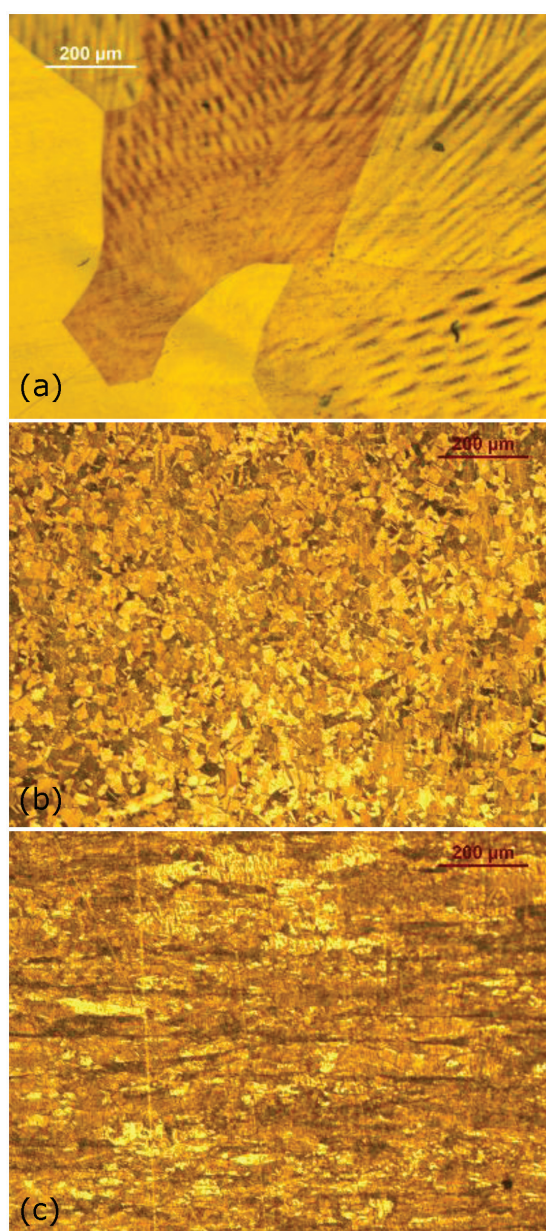


Figure 3: Micrographs of the samples at a 100× magnification: a) rod obtained with upward casting, b) after the extrusion, and c) after the rolling with 80DD

Figure 3c shows that after rolling with an 80 % reduction, visible crystal boundaries are formed and the grains are elongated, i.e., a deformation texture is present. Also, it can be seen that the samples cold rolled in one direction, have grains that are elongated in the direction of rolling, and compressed in the direction normal to the direction of rolling. Cold-deformed samples exhibited good surface conditions, dimensional tolerances, and a uniform structure. Since plastic deformation also increases the internal energy of a crystal, deformed crystals were etched faster than undeformed ones.

Under the effect of Fe, the structure is comminuted and the recrystallization time of Cu is prolonged, thus increasing the mechanical properties, as explained by Rouxel et al.³⁰ and Yu et al.³¹ Their finding was also confirmed in our case.

After each degree of deformation, mechanical characteristics such as hardness, tensile strength, and relative elongation were examined. Their dependence on the degree of deformation and annealing time at a constant temperature is shown in **Figures 4, 5, and 6**.

Based on the obtained results, it can be concluded that at room temperature, with an increase in the degree of deformation, the values for hardness increase proportionally, confirming that the density of dislocations increases significantly with cold deformation. This means that greater deformation leads to an increased dislocation density, causing the formation of grain boundaries that hinder the movement of these dislocations. As a result, higher levels of applied stress are required to continue the deformation process, leading to an increase in the metal hardness.^{32,33} After annealing for 35 min, a sudden drop in the hardness is observed at all degrees of deformation. This annealing time indicates the area of primary recrystallization, characterized by a completely new structure of the crystal lattice that contains defects. In the structure, during recrystallization, elongated grains disappear and new polygonal grains are formed. With a further increase in the annealing time, the hardness values do not change significantly at different degrees of deformation.

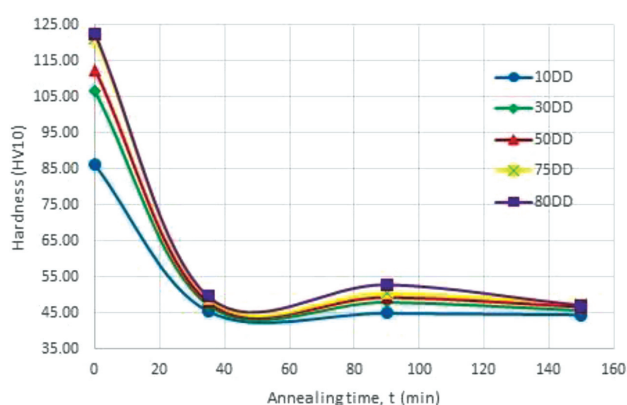


Figure 4: Dependence of hardness on the degree of deformation and annealing time

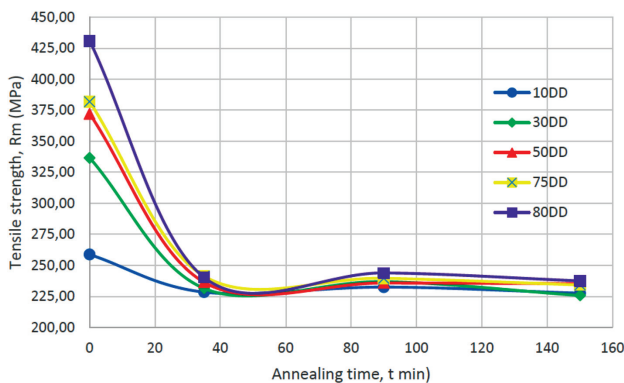


Figure 5: Dependence of tensile strength on the degree of deformation and annealing time

By analyzing the graph that shows the dependence of the tensile strength on the degree of deformation and annealing time, it can be concluded that the tensile strength increases with the increase in the degree of deformation at room temperature. This is because the cold rolled material hardens, increases its strength, and decreases plasticity.³⁴ After annealing for 35 min, there is a sudden drop in the tensile strength for all degrees of deformation, which corresponds to the primary recrystallization. By further extending the annealing time after recrystallization, the tensile strength remains approximately constant at all degrees of deformation.

Considering the dependence of the relative elongation on the degree of deformation and annealing time, presented in **Figure 6**, it was observed that with the increasing of deformation degree, there is a decrease in the relative elongation at room temperature. This is because the material lost its ductility due to cold rolling.³⁵ After annealing for 35 min, the relative elongation increases, while with a further extension of the time, its change is insignificant.

Given that for most of the tested samples, the expected values of the mechanical characteristics are achieved, it remains to demonstrate with the test which samples meet the required structural characteristics, i.e. the number of grains (K_t) per mm^2 under specific

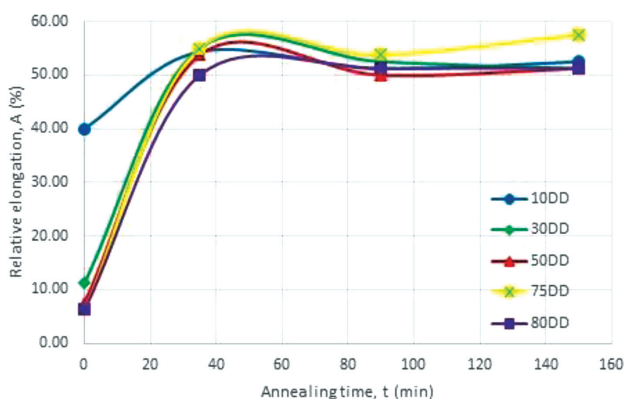


Figure 6: Dependence of relative elongation on the degree of deformation and annealing time

thermomechanical processing conditions. At a small degree of deformation in the metal, there is only a small number of highly deformed places that can recrystallize. The grains formed during annealing in these places grow without significant interfering with each other and, as a result, often reach a considerable size. In a highly deformed metal, on the contrary, there are many deformed regions of the lattice. As a result, during recrystallization, numerous nuclei are formed, from which grains grow. By adding Fe and using the appropriate processing method, their growth is hindered, and a fine-grained recrystallization structure is created.

In addition to the presence of Fe and P, as well as the applied degree of deformation, the size of the grains

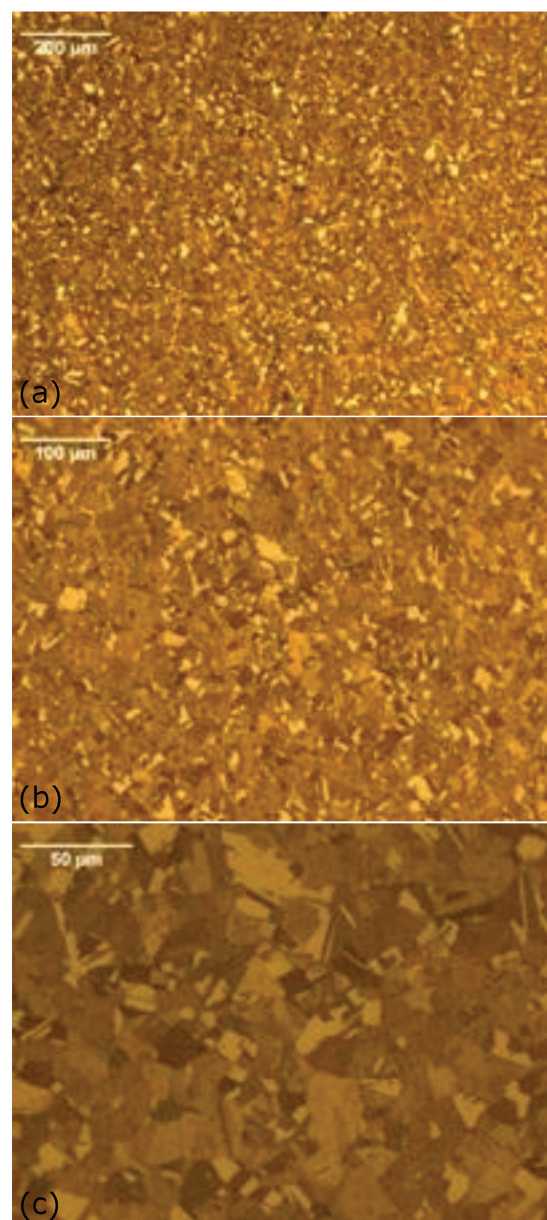


Figure 7: Optical micrographs for sample 80DD-150 at different magnifications: a) magnification of 100x, b) magnification of 200x, c) magnification of 500xh

formed during recrystallization depends on the annealing temperature, annealing time, and cooling rate after annealing. As recrystallized grains are formed similarly to casting grains, through the formation of nuclei and their growth into microscopic or macroscopic grains, similar principles apply to both methods of formation. At shorter annealing times, and higher microscopic magnification, polygonal grains cannot be determined. Prolonging the annealing at the same temperature, as in our case, leads to the formation of numerous very small recrystallized grains. By further prolonging the annealing time, the grains become larger. It follows that a recrystallized grain is larger if a longer annealing time is chosen. However, slow cooling after annealing acts similarly to prolonged annealing time and leads to the formation of larger grains than when cooling is rapid. For this reason, rapid cooling with a solution of water and ethyl alcohol was chosen. It is concluded that the grains formed during recrystallization are finer if there are more impurities, such as the insignificant amount of Fe in our case, i.e., heterogeneously excreted foreign substances in the metal that hinder the grain growth and prolong the recrystallization temperature. Unlike pure Cu, which, after critical deformation recrystallizes with very large grains, Cu alloyed with Fe is quite insensitive to grain growth. In this case, it could be suggested that trace amounts of Fe in Cu prevent the formation of large grains.

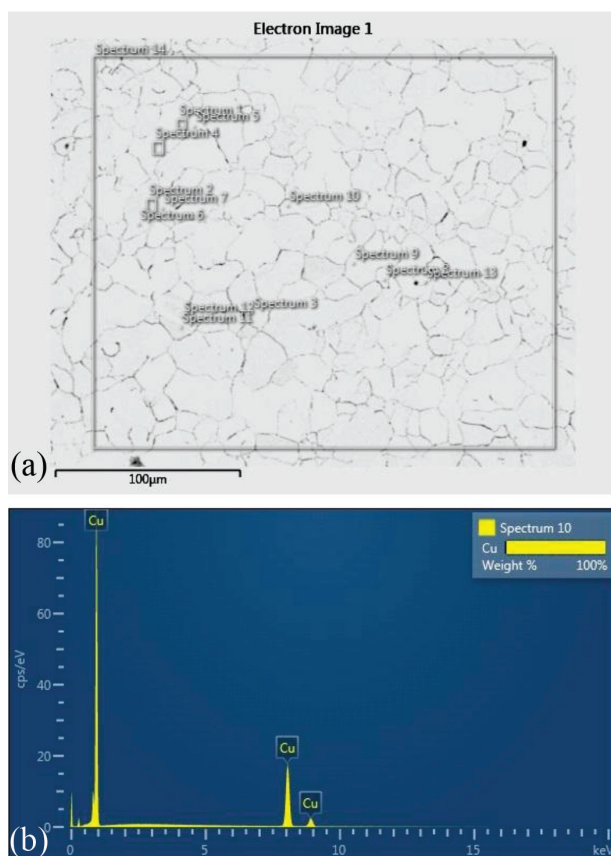


Figure 8: SEM-EDS analysis of sample 80DD-150: a) SEM micrograph at a 200 \times magnification, b) EDS spectrum of point 10

As confirmation of the earlier observation, microalloying Cu with Fe, followed by extrusion, cold processing with a high deformation degree of 80 %, and recrystallization annealing for 150 min, resulted in a very fine-grained structure, shown in **Figure 7**.

Figure 8a shows an SEM micrograph of sample 80DD-150 and 14 points where the same spectral lines were checked and confirmed, as shown in spectrum 10 (**Figure 8b**), being the representative spectrum. Since the investigated Cu-Fe-P alloy contains trace amounts of Fe and P, the EDS (energy dispersive spectrometry) analysis, **Figure 8**, confirmed only the presence of Cu, just like the XRD analysis.

To investigate the distribution of Fe and P phases, an EDS image was obtained by mapping sample 80DD-150, **Figure 9a**. Based on individual images, obtained by elemental mapping, for Cu, Fe, and P, **Figure 9b**, it can be concluded that the distribution of Fe and P is quite balanced, indicating that the alloy is quite homogeneous.

During cold rolling, the grains are elongated along the rolling direction. The level of deformation significantly affects the final grain size after the annealing process. The higher the deformation level, the finer is the grain size after annealing because deformation introduces dislocations and texture into the microstructure. Dislocations introduced by cold rolling provide suitable nucleation sites and are fixed by Fe precipitates, as explained by Dong et al.³⁶ Therefore, higher deformation leads to a higher speed of grain nucleation. Grains are refined after annealing, as explained by Sun and Li³⁷ and Sofyan and Basori,³² which was also demonstrated in our case.

The planimetric method from the ASTM E112-10 standard was used to automatically determine the number of grains.^{25,38} The planimetric method takes into account the grains within a surface that is defined with an

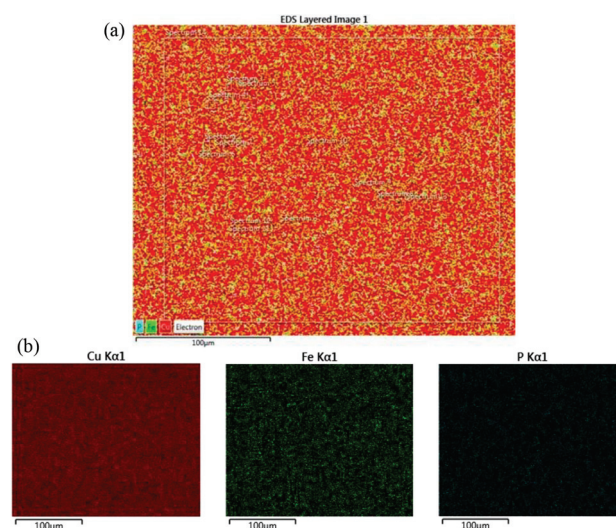


Figure 9: a) EDS analysis of sample 80DD-150 at a 200 \times magnification, b) images of elemental mapping at a 200 \times magnification for Cu, Fe, and P

accuracy of ± 0.25 grain size unit, with the repeatability and reproducibility of grain size units of 0.5. ASTM E112-10 was used as the reference method. **Figure 10** presents a statistical grain count performed using Leica Grain & Phase Expert image analysis software on a selected surface of sample 80DD-150.

The summarized results of the grain count per mm^2 at all DDs and all annealing times, together with the maximum value and standard deviation, are given in **Table 2**. The largest grain count of 4044 belongs to sample 80DD-150. Its main peak is shown in **Figure 10c** and is 9.519; the standard deviation is 1.003, and the minimum grain size is 12.61 μm .

Table 2: Number of grains per mm^2 of all Cu-Fe-P samples with different DDs and different annealing times

Sample	Total count	Mean	St. dev
10DD-35	2454	8.894	± 1.132
10DD-90	2795	9.048	± 1.088
10DD-150	2967	9.135	± 1.095
30DD-35	3258	9.240	± 1.064
30DD-90	3512	9.324	± 1.026
30DD-150	3556	9.367	± 1.070
50DD-35	3526	9.338	± 1.047
50DD-90	3593	9.335	± 1.001
50DD-150	3591	9.350	± 1.036
75DD-35	3539	9.342	± 1.042
75DD-90	3761	9.443	± 1.052
75DD-150	3918	9.474	± 1.011
80DD-35	3793	9.523	± 1.004
80DD-90	3850	9.421	± 0.975
80DD-150	4044	9.519	± 1.003

The histogram in **Figure 10c** has the shape of a Gaussian distribution and represents the grain size distribution. According to the statistics, the limit value (T) is

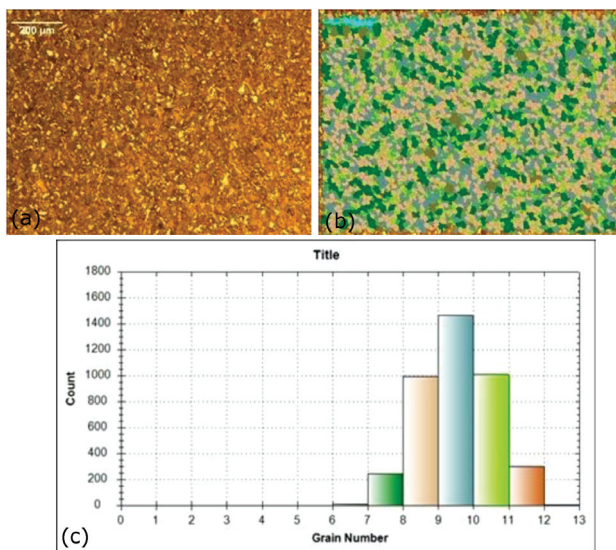


Figure 10: a) Optical micrograph of sample 80DD-150 at a 100 \times magnification, b) grain count statistics, c) grain size distribution histogram

determined at the highest point, and in the case of sample 80DD-150, T is about 9.5. On both sides of the maximum, the number of grains decreases depending on the grain size, as shown on the X-axis.

Based on the results from **Figure 10**, and the values of the number of grains in accordance with the planimetric method, **Table 2**, it can be concluded that only sample 80DD-150 meets the specified structural requirements, including a number of grains of 4044 grains/ mm^2 .

The extruding procedure combined with rolling demonstrated the comminution of the structure of all the examined samples.³⁹ However, higher degrees of deformation (75 % and 80 %) resulted in higher internal stresses as the driving force of the recrystallization process. The higher the level of deformation, the finer is the grain size obtained after annealing. **Table 2** shows that sample 75DD-150 also has a high number of grains, but considering that the tests were carried out at the request of the customer, who expected as fine a structure as possible, the number of grains was the decisive factor for choosing sample 80DD-150 as the representative.

4 CONCLUSIONS

The paper presents the effects of microalloying, extrusion, degree of rolling deformation, temperature, and annealing time on the mechanical and structural characteristics of Cu-based materials developed for the requirements of industry. Based on the obtained results, the following conclusions can be drawn:

Microalloying with iron affected the microstructure comminution, preventing the grain growth and prolonging the recrystallization time, which was the goal of the work;

The extrusion process has proven effective in achieving grain refinement;

Cold plastic processing (rolling) with a high degree of deformation is the third stage in a series of procedures leading to the comminution of a structure. The result of rolling is an increase in the hardness and tensile strength, with a simultaneous decrease in the relative elongation;

At a constant annealing temperature of 450 $^{\circ}\text{C}$, the values of hardness and tensile strength show a sudden drop at the beginning of annealing, while the values of relative elongation increase sharply (up to 35 min). After that, the changes in all the observed quantities become insignificant;

The analysis of the experimental results showed that the optimal conditions for the required mechanical and structural characteristics were achieved at a degree of deformation of 80 %, an annealing time of 150 min, and a temperature of 450 $^{\circ}\text{C}$.

Acknowledgement

The research presented in this paper was done with the financial support from the Ministry of Science and

Technological Development and Innovation of the Republic of Serbia, with the funding by the scientific research work at the Mining and Metallurgy Institute Bor, under Contract No. 451-03-66/2024-03/200052, and the University of Belgrade, Technical Faculty in Bor, in accordance with the contract with Contract No. 451-03-65/2024-03/200131.

5 REFERENCES

- ¹ Y. Zhou, J. Yang, K. Song, S. Yang, Q. Zhu, X. Peng, Y. Liu, Y. Du, S. He, Effect of annealing temperature on dual-structure coexisting precipitates in Cu-2.18Fe-0.03P alloy and softening mechanism at high temperature, *J. Mater. Sci.*, **57** (2022), 20815–20832, DOI: 10.1007/s10853-022-07910-5
- ² J. Zou, D. P. Lu, K. M. Liu, Z. Zhou, Q. F. Fu, Q. J. Zhai, Effect of alternating magnetic field on the microstructure and solute distribution of Cu-14Fe composites, *Mater. Trans.*, **56** (2015), 2058–2062, doi:10.2320/matertrans.m2015244
- ³ M. Wang, R. Zhang, Z. Xiao, S. Gong, Y. B. Jiang, Z. Li, Microstructure and properties of Cu-10 wt%Fe alloy produced by double melt mixed casting and multi-stage thermomechanical treatment, *J. Alloys Compd.*, **820** (2020), 153323, doi:10.1016/j.jallcom.2019.153323
- ⁴ F. Yang, L. M. Dong, L. C. Zhou, N. Zhang, X. F. Zhou, X. D. Zhang, F. Fang, Excellent strength and electrical conductivity achieved by optimizing the dual-phase structure in Cu-Fe wires, *Mater. Sci. Eng. A*, **849** (2022), 143484, doi: 10.1016/j.msea.2022.143484
- ⁵ Y. J. Ding, Z. Xiao, M. Fang, S. Gong, J. Dai, Microstructure and mechanical properties of multi-scale α -Fe reinforced Cu-Fe composite produced by vacuum suction casting, *Mater. Sci. Eng. A*, **864** (2023) 144603, doi:10.1016/j.msea.2023.144603
- ⁶ Y. Z. Tian, S. Y. Peng, Y. Yang, X. Y. Pang, S. Li, M. Jiang, H. X. Li, J. W. Wang, G. W. Qin, Attaining exceptional electrical conductivity in Cu-Fe composite by powder rolling strategy, *Scr. Mater.*, **227** (2023), 115302, doi:10.1016/j.scriptamat.2023.115302
- ⁷ Y. D. Li, X. B. Yuan, B. B. Yang, X. J. Ye, P. Zhang, H. Y. Lang, Q. Lei, J. T. Liu, Y. P. Li, Hierarchical microstructure and strengthening mechanism of Cu-36.8Fe alloy manufactured by selective laser melting, *J. Alloys Compd.*, **895** (2021), 162701, doi:10.1016/j.jallcom.2021.162701
- ⁸ G. A. Jerman, I. E. Anderson, J. D. Verhoeven, Strength and electrical conductivity of deformation-processed Cu-15 Vol Pct Fe alloys produced by powder metallurgy techniques, *Metall. Trans. A.*, **24** (1993), 35–42, doi:10.1007/BF02669600
- ⁹ C. Z. Zhang, C. G. Chen, P. Li, M. J. Yan, Q. Qin, F. Yang, W. W. Wang, Z. M. Guo, A. A. Volinsky, Microstructure and properties evolution of rolled powder metallurgy Cu-30Fe alloy, *J. Alloys Compd.*, **909** (2022), 164761, doi:10.1016/j.jallcom.2022.164761
- ¹⁰ S. F. Abbas, K. T. Park, T. S. Kim, Effect of composition and powder size on magnetic properties of rapidly solidified copper-iron alloys, *Journal of Alloys and Compounds*, **741** (2018), 1188–1195, doi:10.1016/j.jallcom.2018.01.245
- ¹¹ H. Wei, Y. Cui, H. Cui, C. Zhou, L. Hou, Y. H. Wei, Evolution of grain refinement mechanism in Cu-4wt.%Ti alloy during surface mechanical attrition treatment, *Journal of Alloys and Compounds*, **763** (2018), 835–843, doi:10.1016/j.jallcom.2018.06.043
- ¹² Z. L. Li, H. Tian, H. J. Dong, X. J. Guo, X. G. Song, H. Y. Zhao, J. C. Feng, The nucleation-controlled intermetallic grain refinement of Cu-Sn solid-liquid interdiffusion wafer bonding joints induced by addition of Ni particles, *Scripta Materialia*, **156** (2018) 1–5, doi:10.1016/j.scriptamat.2018.07.006
- ¹³ X. H. Feng, Y. J. Li, T. J. Luo, L. H. Li, Y. Wu, M. Zhong, Y. S. Yang, *International Journal of Cast Metals Research*, **30** (2017) 1, 1–5, doi:10.1080/13640461.2016.1158963
- ¹⁴ G. Zaher, I. Lomakin, N. Enikeev, S. Jouen, A. Saiter, X. Sauvage, Influence of strain rate and Sn in solid solution on the grain refinement and crystalline defect density in severely deformed Cu, *Materials Today Communications*, **26** (2021) 101746, doi:10.1016/j.mtcomm.2020.101746
- ¹⁵ G. Chen, K. D. Liss, C. Chen, Y. He, X. Qu, P. Cao, Porous FeAl alloys via powder sintering: Phase transformation, microstructure and aqueous corrosion behavior, *Journal of Materials Science and Technology*, **86** (2021) 64–69, doi:10.1016/j.jmst.2021.01.029
- ¹⁶ L. L. Fang, B. L. Zhang, J. C. Deng, N. Yao, Influence of current density on the characteristics of diamond grains-nickel super-thin cutting blade fabricated by electrotyping, *International Journal of Abrasive Technology*, **1** (2007) 2, 231–238, doi:10.1504/IJAT.2007.015386
- ¹⁷ C. Zhang, C. Chen, R. Ma, M. Yan, H. Zhang, F. Liu, F. Yang, Z. Guo, X. Liu, Simultaneous enhancement of the mechanical and electrical properties of Cu-20Fe alloys by introducing phosphorus, *Materials Characterization*, **209** (2024) 113711, doi:10.1016/j.matchar.2024.113711
- ¹⁸ M. Wang, Y. Jiang, Z. Li, Z. Xiao, S. Gong, W. Qiu, Q. Lei, Microstructure evolution and deformation behaviour of Cu-10wt%Fe alloy during cold rolling, *Materials Science and Engineering: A*, **801** (2021), 140379, doi:10.1016/j.msea.2020.140379
- ¹⁹ M. Wang, R. Zhang, Z. Xiao, S. Gong, Y.B. Jiang, Z. Li, Microstructure and properties of Cu-10wt.%Fe alloy produced by double melt mixed casting and multi-stage thermomechanical treatment, *Journal of Alloy and Compounds*, **820** (2020) 153323, doi:10.1016/j.jallcom.2019.153323
- ²⁰ C.P. Wang, X.J. Liu, Y. Takaku, I. Ohnuma, R. Kainuma, K. Ishida, Formation of core-type macroscopic morphologies in Cu-Fe base alloys with liquid miscibility gap, *Metallurgical & Materials Transactions A*, **35** (2004) 1243-1253, doi:10.1007/s11661-004-0298-y
- ²¹ M. Wang, Y. Jiang, Z. Li, Z. Xiao, S. Gong, W. Qiu, Q. Lei, Microstructure evolution and deformation behaviour of Cu-10wt%Fe alloy during cold rolling, *Materials Science and Engineering: A*, **801** (2021) 140379
- ²² B. Kočovski, Bakar i bakarne legure, Institut za bakar Bor, 1991
- ²³ J. Wang, M. Enomoto, C. Shang, First-principles study on the P-induced embrittlement and de-embrittling effect of B and C in ferritic steels, *Acta Materialia*, **219** (2021) 117260, doi:10.1016/j.actamat.2021.117260
- ²⁴ Y. H. Zhao, Y. Z. Guo, Q. Wei, A. M. Dangelewicz, Y. T. Zhu, T. G. Langdon, E. J. Lavernia, Y. Z. Zhou, C. Xu, Influence of specimen dimensions on the tensile behavior of ultrafine-grained Cu, *Scripta Materialia*, **59** (2008), 627–630, doi:10.1016/j.scriptamat.2008.05.031
- ²⁵ ASTM E112-10: Standard Test Methods for Determining Average Grain Size
- ²⁶ C. Wen, Y. Qiu, Z. Zhang, K. Li, C. Deng, L. Hu, D. Chen, Y. Lu, S. Zhou, Deformation behavior of heterogeneous lamellar Cu-Fe-P immiscible alloys with enhanced strength and ductility produced by laser powder bed fusion, *Journal of Alloys and Compounds*, **971** (2024), 172675, doi:10.1016/j.jallcom.2023.172675
- ²⁷ M. Zhou, X. Yun, H. Fu, Y. Zhang, Y. Liu, A Comparative Study on Flat and U-Shaped Copper Strips Produced by Continuous Extrusion, *Materials*, **15** (2022) 4405, doi:10.3390/ma15134405
- ²⁸ L. P. Lu, X. B. Yun, J. Y. Yang, B. Y. Song, Study on Deforming Behavior of Copper-Magnesium Alloy Wire in Extending Continuous-Extrusion Process, *Hot Working Technology*, **39**, (2010), 92–95
- ²⁹ S. Qu, X. H. An, H. J. Yang, C. X. Huang, G. Yang, Q. S. Zang, Z. G. Wang, S. D. Wu, Z. F. Zhang, Microstructural Evolution and Mechanical Properties of Cu-Al Alloys Subjected to Equal Channel Angular Pressing, *Acta Materialia*, **57** (2009) 5, 1586–1601, doi:10.1016/j.actamat.2008.12.002
- ³⁰ B. Rouxel, C. Cayron, J. Bornand, P. Sanders, E.R. Logé, Micro-addition of Fe in highly alloyed Cu-Ti alloys to improve both

- formability and strength, *Materials & Design*, 213 (2022), 110340, doi:10.1016/j.matdes.2021.110340
- ³¹ H. Yu, Y. Zeng, R. Hong, Influence of Fe Addition on the Microstructure and Mechanical Properties of Cu Alloys, *Material Sci.*, 3 (2021) 1, 10, doi:10.35702/msci.10010
- ³² B. T. Sofyan, I. Basori, Effects of deformation and annealing temperature on the microstructures and mechanical properties of CU-32%ZN brass, *ARP Journal of Engineering and Applied Sciences*, 11 (2016) 4, 2741–2745
- ³³ R. Markandeya, S. Nagarjuna, D. Sarma, Effect of prior cold work on age hardening of Cu-3Ti-1Cr alloy, *Materials Characterization*, 57 (2006) 4–5, doi:10.1016/j.matchar.2006.02.017
- ³⁴ H. Y. Chao, H. F. Sun, E. D. Wang, Working hardening behaviors of severely cold deformed and fine-grained AZ31 Mg alloys at room temperature, *Transactions of Nonferrous Metals Society of China*, 21 (supp-S2) (2011), doi:10.1016/S1003-6326(11)61584-7
- ³⁵ W. Horizon, S. K. Nisa, B. T. Sofyan, Effect of Cold Rolling and Annealing Temperature on the Characteristics of Cu-28Zn-3.2Mn Alloy, *Materials Science and Engineering*, 517 (2019), 012002, doi:10.1088/1757-899X/517/1/012002
- ³⁶ Q. Dong, L. Shen, M. Wang, Y. Jia, Z. Li, F. Cao, C. Chen, Microstructure and properties of Cu-2.3Fe-0.03P alloy during thermomechanical treatments, *Trans. Nonferrous Met. Soc. China*, 25 (2015), 1551–1558, doi:10.1016/S1003-6326(15)63757-8
- ³⁷ S. Sun, T. Li, Effect of cold rolling process on microstructure and properties of T1 copper sheet, *Journal of Physics: Conference Series*, 1605 (2020), 012132, doi:10.1088/1742-6596/1605/1/012132
- ³⁸ H. Peregrina-Barreto, I. R. Terol-Villalobos, J. J. Rangel-Magdaleno, A. M. Herrera-Navarro, L. A. Morales-Hernández, F. Manríquez-Guerrero, Automatic grain size determination in microstructures using image processing, *Measurement*, 46 (2013) 249–258
- ³⁹ X. Yuna, M. Zhou, T. Tian, Y. Zhao, Continuous extrusion and rolling forming technology of copper strip manufacture, *MATEC Web of Conferences*, 21 (2015), 03004, doi:10.1051/mateconf/20152103004